Geophysical Research Letters

RESEARCH LETTER
10.1029/2018GL081585

**Key Points:**
- Global survey demonstrates a correlation between bending faults in the incoming plate and the seismicity rate of intermediate-depth earthquakes
- Fault throw provides a proxy for overall fault damage and the ability of water to penetrate and hydrate the incoming plate
- A mechanical parameter based on the incoming plate faulting controls the seismicity rate of intermediate-depth earthquakes

**Supporting Information:**
- Supporting Information S1
- Figure S1
- Figure S2
- Figure S3
- Figure S4
- Figure S5
- Figure S6

**Correspondence to:**
Y. Boneh,
bonehyuv@bgu.ac.il

**Citation:**
Boneh, Y., Schottenfels, E., Kwong, K., van Zelst, I., Tong, X., Eimer, M., et al. (2019). Intermediate-depth earthquakes controlled by incoming plate hydration along bending-related faults. *Geophysical Research Letters*, *46*. https://doi.org/10.1029/2018GL081585

Received 4 DEC 2018
Accepted 19 MAR 2019
Accepted article online 22 MAR 2019



# Intermediate-Depth Earthquakes Controlled by Incoming Plate Hydration Along Bending-Related Faults

**Yuval Boneh[1,2], Emily Schottenfels[3], Kevin Kwong[4], Iris van Zelst[5], Xinyue Tong[6], Melody Eimer[7], Meghan S. Miller[8], Louis Moresi[9], Jessica M. Warren[10], Douglas A. Wiens[7], Magali Billen[11], John Naliboff[11], and Zhongwen Zhan[12]**

[1]Department of Geological Sciences, Brown University, Providence, RI, USA, [2]Now at Department of Geological and Environmental Sciences, Ben-Gurion University of the Negev, Be'er-Sheva, Israel, [3]Department of Earth and Environment, Boston University, Boston, MA, USA, [4]Roy M. Huffington Department of Earth Science, Southern Methodist University, Dallas, TX, USA, [5]Seismology and Wave Physics, Institute of Geophysics, Department of Earth Sciences, ETH Zürich, Zürich, Switzerland, [6]Department of Geological Sciences, Jackson School of Geosciences, University of Texas at Austin, Austin, TX, USA, [7]Department of Earth and Planetary Sciences, Washington University in St. Louis, Saint Louis, MO, USA, [8]Research School of Earth Sciences, Australian National University, Canberra, ACT, Australia, [9]School of Earth Sciences, University of Melbourne, Parkville, Victoria, Australia, [10]Department of Geological Sciences, University of Delaware, Newark, DE, USA, [11]Department of Geology, University of California, Davis, CA, USA, [12]Seismological Laboratory, Division of Geological and Planetary Sciences, California Institute of Technology, Pasadena, CA, USA

**Abstract** Intermediate-depth earthquakes (focal depths 70–300 km) are enigmatic with respect to their nucleation and rupture mechanism and the properties controlling their spatial distribution. Several recent studies have shown a link between intermediate-depth earthquakes and the thermal-petrological path of subducting slabs in relation to the stability field of hydrous minerals. Here we investigate whether the structural characteristics of incoming plates can be correlated with the intermediate-depth seismicity rate. We quantify the structural characteristics of 17 incoming plates by estimating the maximum fault throw of bending-related faults. Maximum fault throw exhibits a statistically significant correlation with the seismicity rate. We suggest that the correlation between fault throw and intermediate-depth seismicity rate indicates the role of hydration of the incoming plate, with larger faults reflecting increased damage, greater fluid circulation, and thus more extensive slab hydration.

**Plain Language Summary** In subduction zones, one tectonic plate plunges beneath another into the Earth's interior. Some of the earthquakes that occur at subduction zones are unusual due to their occurrence at depths of 70 to 300 km (*intermediate depths*), deeper than the expected limit of brittle failure. In this study, we evaluate whether the faults that form when a plate bends as it enters a subduction zone can explain the occurrence of these deep earthquakes. Sea water penetrates deep into these faults and forms new, hydrous minerals, but these new minerals are not stable deeper in the subduction zone. Laboratory experiments show that breakdown of these hydrous minerals can cause seismicity at depths of 70–300 km (intermediate depths). Here we examined a set of 17 subduction zone segments around the globe and found that the seismicity is correlated with the faults that formed due to plate bending. This observation can be explained if the amount of faulting prior to subduction controls the amount of hydrous mineral formation, which subsequently determines the intensity and rate of subduction zone-related intermediate-depth earthquakes.

## 1. Introduction

Intermediate-depth earthquakes, defined as seismic events at depths of 70–300 km, are a unique feature of subduction zones, delineating the upper crust and mantle of the subducting slab in what is often referred to as the Wadati-Benioff zone (Benioff, 1963; Wadati, 1928). The dehydration of hydrous minerals in the subducted slab is the most commonly invoked mechanism to explain events at these depths, where conditions of high temperature and pressure should inhibit dynamic fracture or frictional sliding (Green & Houston, 1995; Hirth & Guillot, 2013; Meade & Jeanloz, 1991; Yamasaki & Seno, 2003). Rheological instabilities in some hydrous minerals deformed under high pressures (>1 GPa) have been observed experimentally (Ferrand et al., 2017; Jung et al., 2004, 2009; Okazaki & Hirth, 2016; Proctor & Hirth, 2016; Raleigh & Paterson,

1965). However, there is still ambiguity regarding the specific mechanism(s) through which hydrous minerals can generate seismic events. Additionally, there is considerable uncertainty about the degree of hydration of the incoming plate, particularly for the oceanic upper mantle, which should be largely anhydrous due to extraction of water during mid-ocean ridge melting (e.g., Hacker, 2008).

Extensional faulting due to plate bending provides a conduit for fluids into the crust and uppermost mantle. Slab hydration and fluid circulation associated with plate bending-related faults have been observed in seismic and electromagnetic studies (Cai et al., 2018; Grevemeyer et al., 2007; Key et al., 2012; Nedimović et al., 2009; Van Avendonk et al., 2011; Worzewski et al., 2011). Numerical models suggest that stress and pressure changes during slab bending and slab unbending can induce circulation of fluid through the fault zones into the lithospheric mantle (Faccenda et al., 2009, 2012). Subducting slabs have been inferred to contain a significant amount of water, with hydration of the crust and mantle deduced from seismic surveys (Abers, 2000; Cai et al., 2018; Faccenda et al., 2008; Peacock, 1990; Pozgay et al., 2009; Zhao et al., 2007) and from chemical enrichments observed in arc magmas (e.g., Plank & Langmuir, 1998; Stern, 2002).

This wide range of observations for incoming plate hydration, together with the experimental evidence for embrittlement of hydrous minerals at high pressures, leads to an expected relationship between incoming plate bending faults, amount of slab hydration, and intermediate-depth seismicity (Ranero et al., 2005). A correlation between the hydration state of the incoming plate and the seismicity rate in the subducted slab has been established regionally (Shillington et al., 2015). However, a previous attempt to find a worldwide relationship based on the predicted water flux due to mineral dehydration did not find a correlation (Barcheck et al., 2012). Here we show that incoming plate faults, which may control the extent of hydration pathways in the subducted slab, correlates globally with the off-trench intermediate-depth earthquakes. We postulate that the global distribution of intermediate-depth earthquakes is controlled by the extent of faulting and fracturing on the incoming plate, and thus, that hydration is inherited through the brittle deformation history of the incoming plate.

## 2. Methods

### 2.1. Seismicity Rate for Intermediate Depth Earthquakes

In order to quantify the seismic productivity of intermediate-depth earthquakes, we used the International Seismological Centre (ISC) Bulletin earthquake catalog (http://www.isc.ac.uk). The ISC Bulletin is the most complete and comprehensive teleseismic earthquake catalog available and includes documentation of globally recorded earthquake hypocenters, phases, magnitudes, and other pertinent earthquake data (e.g., Di Giacomo et al., 2015).

The intermediate-depth events used in this study were chosen based on three criteria: (1) focal depth of 70–300 km, (2) magnitude of $m_b \geq 4.5$, and (3) occurrence between 1964 to 2015. Although the ISC catalog contains events beginning in 1900, global monitoring of earthquakes for these magnitudes became effective only in the 1960s. We define the seismicity rate as the number of events normalized by the trench length (km) and time (year).

We estimated the seismicity rate for 17 subduction zone segments (Figure 1) with trench lengths of 210–1,450 km (Table S1 in the supporting information). For each segment, the increasing focal depth of intermediate-depth events away from the trench traces the descending slab. Maps of each subduction zone showing the trench segments are provided in Figure S1 in the supporting information.

### 2.2. Bending-Related Fault Throw

Slab flexure and the resulting tensional stresses generate normal faulting (e.g., Ludwig et al., 1966; Parsons & Molnar, 1976; Ranero et al., 2003). The bending-related normal faults, manifested in horst and graben features, are a common characteristic of subduction zones and can be seen in seismic reflection images and bathymetric maps up to about 100 km seaward of the trench axis (e.g., Chapple & Forsyth, 1979; Hilde, 1983).

We quantified the vertical component of fault displacement (i.e., fault throw) in the incoming plate using a compilation of previously published bathymetry data from seismic reflection imaging and ship-based multibeam mapping (Table S2). In regions with sparse or no data for bending fault offset, we used bathymetric

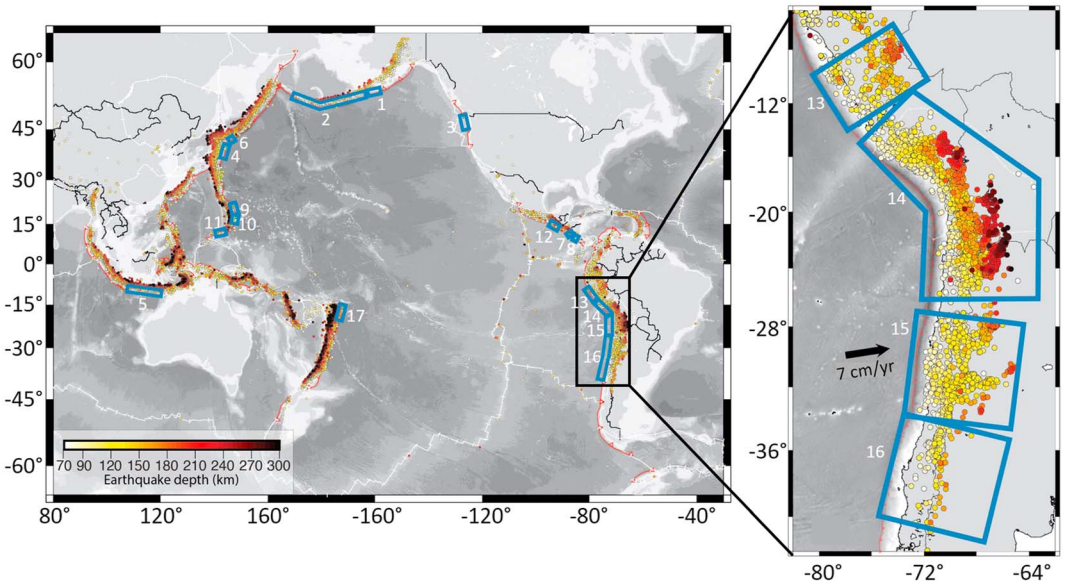


**Figure 1.** (left) Global map showing the subduction zone segments used in this paper (segment numbers correspond to IDs in Table S1). Intermediate-depth earthquakes are delineated by circles colored by the hypocenter depth. (right) Enlargement of the South-America trench, subdivided into four segments of different seismicity rates.

data from the Global Multi-Resolution Topography (Ryan et al., 2009) accessed with GeoMapApp (http://www.geomapapp.org/). Topographic profiles orthogonal to both fault strike and the trench were manually selected and used to calculate the vertical fault throw on distinct seaward facing normal faults (Figures 2 and S2). We quantified the maximum fault throw (MFT) for each region as a representation of the regional faulting intensity. Here we focus on MFT calculated as the average of the largest 10% of fault throw measurements for each region, but we also evaluated MFT based on the largest 5%, 20%, and 30% of fault throw measurements (Figure S3).

Fault throw represents fault displacement when a small variation in dip angle is assumed. We use it here to represent fault intensity on the assumption that this provides a proxy for hydration of the incoming plate. We therefore omit bathymetry related to seamounts and focus on bathymetry related to plate faulting.

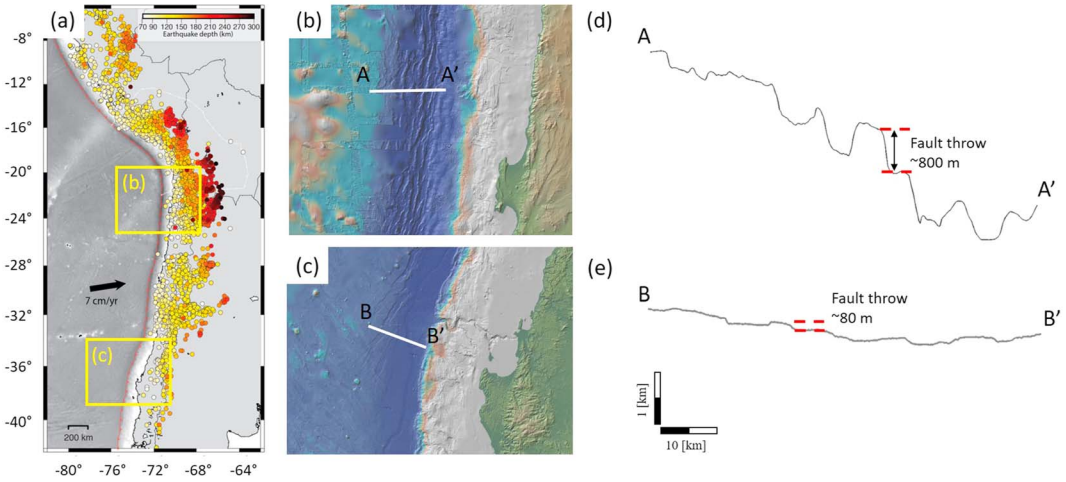


**Figure 2.** Bathymetry and incoming plate roughness due to bending faults. (a) The South American coast with intermediate-depth earthquakes (from Figure 1). The yellow boxes show the locations of the zoomed-in bathymetry images shown in b and c. (b and c) Bathymetric maps (Global Multi-Resolution Topography) where A-A′ and B-B′ indicate the cross sections in d and e, respectively, showing the rough central (b) and conversely smooth southern (c) bathymetry off South America.

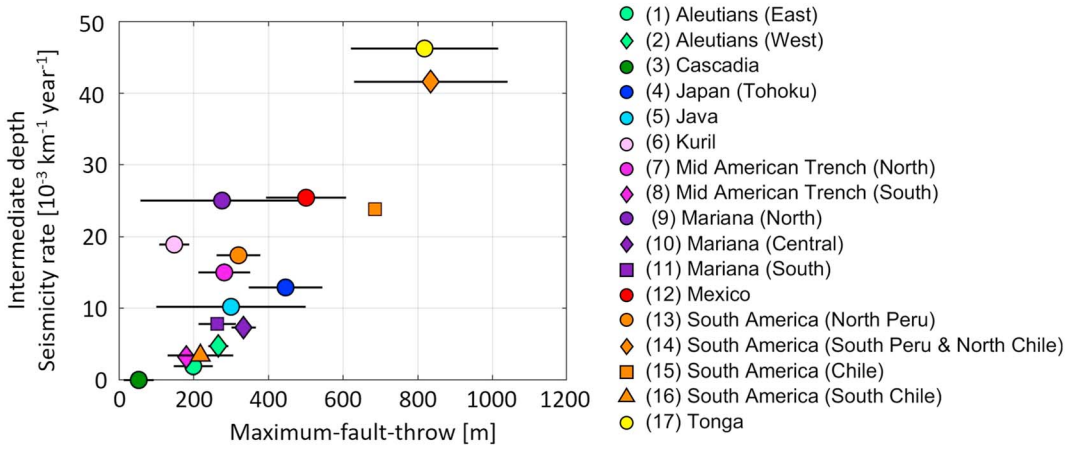


**Figure 3.** The seismicity rate of intermediate-depth earthquakes against the incoming plate maximum fault throw. Maximum fault throw error bars are the standard deviation of the averaged 10% fraction of the largest fault throws, except Java, which is estimated to be 100–500 m by Masson (1991). The error bars for segment 15 are smaller than the symbol size.

Topographic fault scarps and fault throw estimates have often been used to infer regional stress state, tectonics, and deformation rates where direct field studies are not possible, such as is in other submarine environments and planets (Schultz et al., 2006; Wilkins et al., 2002).

## 3. Results

### 3.1. Comparison of Incoming Plate Properties With Seismicity Rate

The covariation of the bathymetric expression of faults (as represented by MFT), and the intermediate-depth seismicity rate for the 17 trench segments, is shown in Figure 3. This correlation suggests a general trend, where the largest fault throws are associated with an increase in intermediate-depth seismicity. For example, the bathymetry of Cascadia presents low fault throw values of less than 50 m (Masson, 1991) and no intermediate-depth earthquakes have been recorded at this subduction zone. On the other hand, the highly faulted slab at the Tonga trench has the highest seismicity rate of our data set ($46.2 \cdot 10^{-3}$ km$^{-1}$ year$^{-1}$). Regional data show a similar trend. For example, we divided the Nazca plate, which subducts beneath South America, into four parts according to the bathymetric texture (Figure 1). Along the northern part of the South America trench, the bathymetry is rough with MFT ~ 800 m, whereas the ocean-floor becomes smoother toward the south with MFT ~ 80 m (Figure 2). The seismicity rate follows this trend, with higher seismicity rates corresponding to regions with rougher fault scarps. To test possible variations in the magnitude completeness of the ISC seismic catalog, we compared the seismicity rate with a threshold of $m_b \geq 4.5$ and threshold of $m_b \geq 5.6$ (Di Giacomo et al., 2015). We found no significant statistical difference in the seismicity rate between the two thresholds (Figure S4).

Syracuse et al. (2010) defined several slab properties, and the correlation of these properties with seismicity rate is shown in Figure 4; slab age (Figure 4a), convergence velocity (Figure 4b), dip angle (Figure 4c), and thermal parameter (Figure 4d). In contrast to the positive trend between MFT and seismicity rate, none of these parameters show a clear correlation with intermediate-depth earthquake intensity. In particular, the thermal parameter ($\varphi$) is defined as the product of slab age and convergence velocity perpendicular to the trench (Kirby et al., 1996), where higher values of $\varphi$ correspond to cooler slabs. This parameter provides a proxy for slab temperature, assuming that heating of the subducting lithosphere is by conduction (Molnar et al., 1979). The thermal state of a subduction zone has been assumed to control deep seismicity due to temperature-dependent mineral breakdowns reactions (Kirby et al., 1991), yet $\varphi$ is not correlated with seismicity rate (Figure 4d).

### 3.2. Statistical Significance of the MFT Correlation With Seismicity Rate

We use three different statistical measures to evaluate the correlations between MFT and properties of the incoming plate (Table S3): (1) the Pearson product-moment correlation coefficient, (2) the Kendall rank

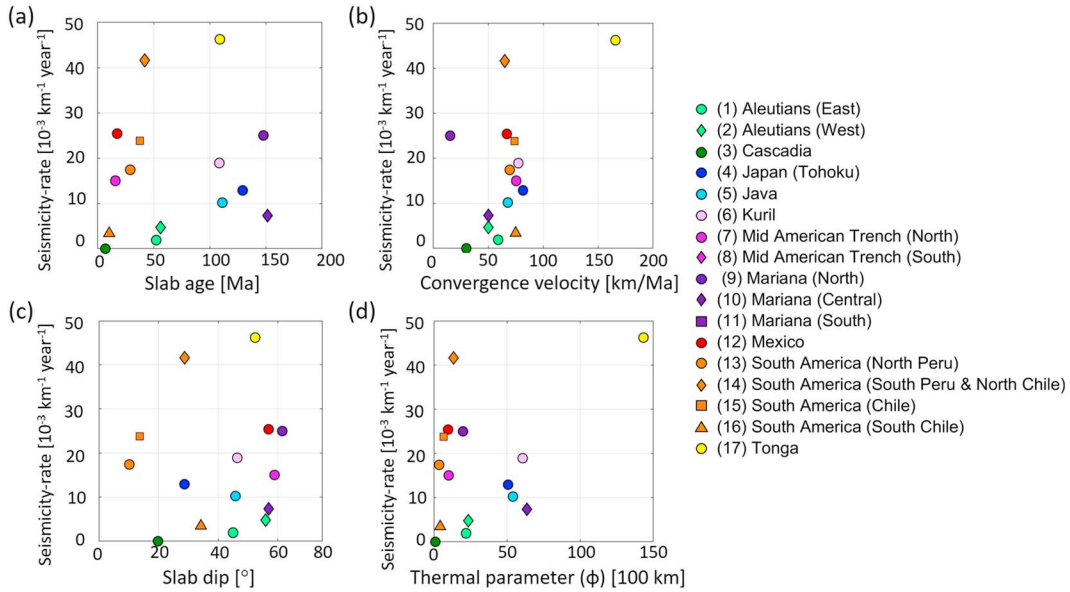


**Figure 4.** The seismicity rate of intermediate-depth earthquakes plotted against slab properties from Syracuse et al. (2010): (a) age, (b) convergence velocity, (c) dip angle, and (d) thermal parameter.

correlation coefficient, and (3) the Spearman rank correlation coefficient. The Pearson's coefficient is used to explore the linear dependence between two variables. The other two coefficients provide a measure of how well the relationship between the two variables can be described by a monotonic function. In other words, they test the extent to which the positive/negative relationship between two variables is systematic without the necessity of a linear relationship. We also calculated the *p*-value to test the significance of the correlations, where $p$ varies between 0 and 1 and a small *p*-value indicates evidence against the null hypothesis. In our analyses, the null hypothesis is that no correlation exists between the two variables. We consider a correlation to be significant when $p \ll 0.05$ and when the correlation coefficients are higher than ~0.6.

Our analysis reveals high, statistically significant correlations between seismicity rate and MFT for all three statistical tests (Figure S5). The correlation between seismicity rate and MFT (average of the top 10% of fault throws) shows values of 0.86, 0.6, and 0.74 for the Pearson, Kendall, and Spearman coefficients, respectively (Table S3). In contrast, none of the four other parameters (slab age, velocity, dip, and thermal parameter) show a significant correlation, with coefficients <0.54, 0.21, and 0.32 for the Pearson, Kendall, and Spearman coefficients, respectively (Figure S4). We also tested different definitions for MFT, using both higher (20% and 30%) and lower (5%) percentages of the total fault throw to calculate MFT. The correlation of seismicity rate with MFT is statistically significant for all definitions although using a higher percentage (20 or 30% of the largest faults throws) results in slightly lower correlations.

The rank correlation coefficients (Kendall and Spearman) give slightly lower correlations than the linear correlation coefficient (Pearson), because they are less sensitive to extreme values. The high value of the Pearson coefficient partly stems from the high MFT and seismicity rate values Tonga and South Peru-North Chile. Nevertheless, the fact that the rank dependence coefficients also show significant correlations supports our finding of a positive relationship between MFT and seismicity rate.

## 4. Discussion

Our results indicate that bending-related faulting of the incoming plate may have a significant control on the seismicity rate of intermediate-depth earthquakes. This relationship between shallow incoming plate faults and intermediate-depth seismicity rate was previously shown for the Nazca and Cocos plates and was interpreted as fault reactivation (Ranero et al., 2005). However, Warren et al. (2007, 2008) found that rupture directivity of intermediate-depth earthquakes was inconsistent with the orientation of outer-rise normal

faults. Thus, the correlation that we observe may instead be explained by hydration along these faults, with subsequent embrittlement of the hydrated regions at >70 km, in accordance with nucleation mechanisms for intermediate-depth earthquakes.

### 4.1. Fault-Zone Damage Leads to Slab Hydration

Bending faults provide a pathway for fluid circulation and deep hydration within the downgoing plate (Emry & Wiens, 2015; Grevemeyer et al., 2007; Iyer et al., 2012; Key et al., 2012; Nishikawa & Ide, 2015; Ranero et al., 2003; Ranero & Sallares, 2004; Tilmann et al., 2008). The damage associated with faulting leads to channels of increased permeability that allow deep fluid penetration into the oceanic lithosphere (e.g., Naif et al., 2015), and these fluids react with the host rock to form hydrous minerals (e.g., Andreani et al., 2007). The ability of fluids to penetrate and react deep in the lithosphere is governed by properties such as fracture density, permeability, and porosity, which are enhanced by faulting (Sibson, 2000). Importantly, these physical properties are expected to evolve through progressive displacement on faults.

Fault displacement and length scaling relationships (Cowie & Scholz, 1992; Schultz et al., 2006) suggest that for greater fault displacement (and therefore greater fault throw), a larger volume of the incoming plate is damaged. This provides the potential for enhanced hydration on larger faults, and thus, more hydrous minerals would then be available at intermediate depths to cause dehydration embrittlement. Gouge thickness (Scholz, 1987) and damage zone (DZ) thickness (Faulkner et al., 2011; Savage & Brodsky, 2011; Shipton & Cowie, 2001) increase with increased fault displacement. Hence, the ability of fluids to migrate through the rock is dependent on the DZ structure. Within the core of a fault, the permeability may be low due to the presence of fault gouge. However, in material adjacent to the fault core, the permeability can be an order of magnitude higher as a result of cracking in the region known as the DZ (Caine et al., 1996; Evans et al., 1997).

Mitchell and Faulkner (2012) showed that fracture density, DZ width, and fault displacement control overall DZ permeability and that fault-related fracturing and permeability scale with fault displacement. The displacement ($d$) is scaled with the width of damage surrounding the fault (DW):

$$\mathrm{DW} = \frac{a\,d}{b + d} \tag{1}$$

where DW is in meters and $a$ and $b$ are constants with values of 96.25 and 147.16, respectively (Mitchell & Faulkner, 2012; Savage & Brodsky, 2011) based on regression of fault-zone data (Faulkner et al., 2011). Cowie and Scholz (1992) showed that the fault length ($L$) can be scaled with the displacement:

$$d/L \propto 0.01 \tag{2}$$

Assuming Andersonian faults with 60° dip, displacement can be estimated from the fault throw. Using equations (1) and (2), the area of the DZ due to faulting can be estimated:

$$\mathrm{DZ} = L \cdot \mathrm{DW} \tag{3}$$

where DZ has units of $m^2$. The faults related DZ increases the permeability around the fault and allows fluid infiltration and subsequent hydration (Reynolds & Lister, 1987; Rüpke & Hasenclever, 2017).

For the bending faults in this study, the DZ width, estimated from the fault-throw, shows a quasi-linear relationship with the seismicity rate (Figure 5). As hydration kinetics are relatively fast (Martin & Fyfe, 1970), the limiting factor for slab hydration is the supply of water through brittle slab fractures and faults (Rüpke et al., 2013). Although mineral production during hydration reactions has the potential to seal cracks (e.g., Michibayashi et al., 2008), the reaction also results in a positive volume change that can generate additional fracturing and permeability (Audet et al., 2009; Jamtveit et al., 2009). The relationship between mechanical faulting and the extent of plate hydration has been observed in extensional faults at continental rifts (Pérez-Gussinyé & Reston, 2001), where faults have been found to serve as fluid conduits for hydration. Bayrakci et al. (2016) used seismic tomography of a continental margin offshore from western Spain to determine that the volume of serpentine had a linear dependence with the amount of fault displacement, consistent with the linear relationship presented in this study (Figure 5). We conclude that fault displacement

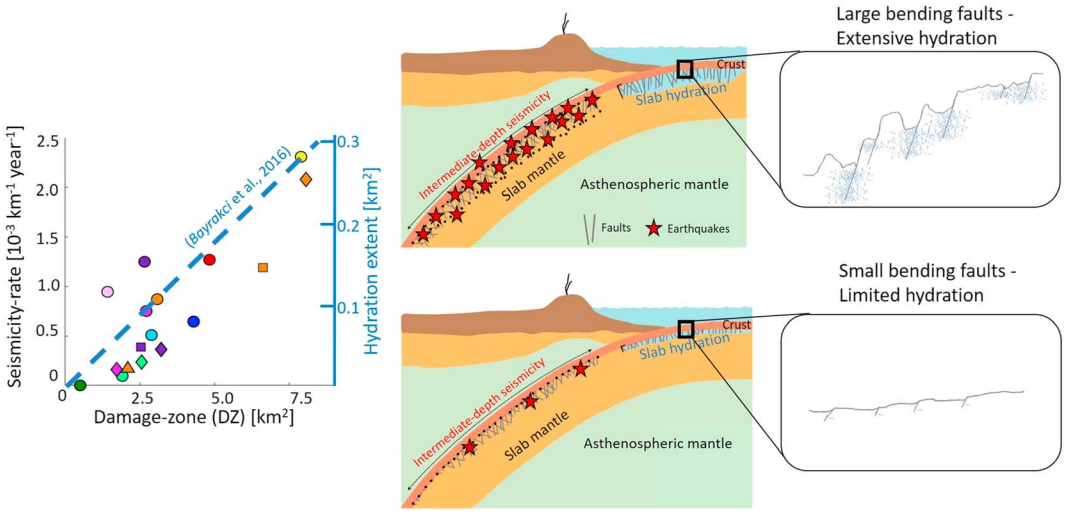


**Figure 5.** (left) Seismicity rate plotted against damage-zone width estimated from fault displacements. Data from this study show a similar relationship to the estimated extent of hydration as a function of damage-zone width as determined from seismic data by Bayrakci et al. (2016) for the Iberia rifted margin. (right) Schematic diagram of a subduction zone, illustrating the relationship between bending faulting, incoming plate hydration, and intermediate-depth seismicity (modified from Billen, 2009).

controls the overall DZ structure and permeability of the subducted plate and that bending faults function as conduits for fluid infiltration into the oceanic lithosphere. Therefore, MFT provides a proxy for the extent of hydration in the slab, which later leads to intermediate-depth seismicity.

### 4.2. The Effect of Incoming Plate Structure on Intermediate Depth Earthquakes

Previous studies have investigated the relationship between the thermal structure of the slab, dehydration, and intermediate-depth seismicity (Abers et al., 2013; Hacker et al., 2003; van Keken et al., 2011; Wei et al., 2017). The premise behind such studies is that dehydration and breakdown of hydrous minerals cause intermediate-depth seismicity, as the thermo-petrological state of the slab determines when mineral phase boundaries are crossed, controlling the depth of earthquakes (Gorbatov & Kostoglodov, 1997; Hacker et al., 2003; Peacock, 2001). Fracturing, elevated fluid pressure, and stress heterogeneities due to dehydration may all contribute to the nucleation of intermediate-depth earthquakes (Davies, 1999; Ferrand et al., 2017; Gasc et al., 2017).

The correlation of thermal structure and slab age with intermediate-depth seismicity suggests that the nucleation mechanism is temperature dependent (Brudzinski et al., 2007). This could be associated with the specific rheology of the hydrous minerals that have formed due to the brittle-ductile-brittle transitions characteristic of many hydrous minerals (Brantut et al., 2011; Jung et al., 2009; Proctor & Hirth, 2016; Raleigh & Paterson, 1965). Alternatively, seismicity may result from dehydration embrittlement and the related change of fluid pressure and stress heterogeneities (Ferrand et al., 2017; Hirth & Guillot, 2013; Okazaki & Hirth, 2016). Although the pressure-temperature conditions in the slab are a first-order control on the release of fluids at intermediate depths, here we find that a mechanical parameter, fault throw, determines the net availability of fluids and therefore controls the intensity of intermediate-depth seismicity.

## 5. Conclusions

We show a significant correlation between a global data set of intermediate-depth seismicity rates and the occurrence of shallow faulting caused by plate bending. Other parameters of the subducted slab such as plate age, convergence velocity, dip angle, and thermal parameter do not show a statistically significant correlation. Our results suggest that shallow processes associated with bending faults of the incoming plate have a strong control over intermediate-depth seismicity rate. We propose that the hydration extent of the subducted slab, estimated from its faulting, exerts a primary control on the prevalence of intermediate-depth seismicity. Thermo-petrological models that seek to describe intermediate-depth earthquakes through

mineral phase stability and breakdown of hydrous phases should also account for the extent of hydration within the slab.

**Acknowledgments**
This research project was initiated at the 2017 Cooperative Institute for Dynamic Earth Research (CIDER) summer program "Subduction Zone Dynamics" at the University of California, Berkeley. We wish to thank the other organizers B. Romanowicz, P. van Keken, E. Hauri, and C. Till. CIDER-II is funded as a "Synthesis Center" by the Frontiers of Earth Systems Dynamics (FESD) program of NSF under grant number EAR-1135452. We also wish to thank Geoffrey Abers and an anonymous reviewer for constructive comments and gratefully acknowledge Yi Hu, Wang-Ping Chen, Samer Naif, and Hannah Rabinowitz for valuable discussions. Bathymetry profiles from GeoMapApp (http://www.geomapapp.org/) were used in this study and are included in the supporting information. A bathymetry profile from the Mariana trench (center) was collected by R/V Langseth cruise, MGL1204, and is available from NOAA at http://www.marine-geo.org/link/entry.php?id=MGL1204. Seismic data for the Japan trench were collected by JAMSTEC (KR13-11). Seismicity data used to quantify the intermediate-depth seismicity rate were taken from the International Seismological Centre (ISC) Bulletin earthquake catalog (http://www.isc.ac.uk).

## References

Abers, G. A. (2000). Hydrated subducted crust at 100–250 km depth. *Earth and Planetary Science Letters*, *176*(3–4), 323–330.
Abers, G. A., Nakajima, J., van Keken, P. E., Kita, S., & Hacker, B. R. (2013). Thermal–petrological controls on the location of earthquakes within subducting plates. *Earth and Planetary Science Letters*, *369*, 178–187.
Andreani, M., Mével, C., Boullier, A. M., & Escartin, J. (2007). Dynamic control on serpentine crystallization in veins: Constraints on hydration processes in oceanic peridotites. *Geochemistry, Geophysics, Geosystems*, *8*, Q02012. https://doi.org/10.1029/2006GC001373
Audet, P., Bostock, M. G., Christensen, N. I., & Peacock, S. M. (2009). Seismic evidence for overpressured subducted oceanic crust and megathrust fault sealing. *Nature*, *457*(7225), 76.
Barcheck, C. G., Wiens, D. A., van Keken, P. E., & Hacker, B. R. (2012). The relationship of intermediate-and deep-focus seismicity to the hydration and dehydration of subducting slabs. *Earth and Planetary Science Letters*, *349*, 153–160.
Bayrakci, G., Minshull, T., Sawyer, D., Reston, T. J., Klaeschen, D., Papenberg, C., et al. (2016). Fault-controlled hydration of the upper mantle during continental rifting. *Nature Geoscience*, *9*(5), 384.
Benioff, H. (1963). Source wave forms of three earthquakes. *Bulletin of the Seismological Society of America*, *53*(5), 893–903.
Billen, M. I. (2009). Tectonics: Soaking slabs. *Nature Geoscience*, *2*(11), 744.
Brantut, N., Schubnel, A., & Guéguen, Y. (2011). Damage and rupture dynamics at the brittle-ductile transition: The case of gypsum. *Journal of Geophysical Research*, 116, B01404. https://doi.org/10.1029/2010JB007675
Brudzinski, M. R., Thurber, C. H., Hacker, B. R., & Engdahl, E. R. (2007). Global prevalence of double Benioff zones. *Science*, *316*(5830), 1472–1474.
Cai, C., Wiens, D. A., Shen, W., & Eimer, M. (2018). Water input into the Mariana subduction zone estimated from ocean-bottom seismic data. *Nature*, *563*(7731), 389.
Caine, J. S., Evans, J. P., & Forster, C. B. (1996). Fault zone architecture and permeability structure. *Geology*, *24*(11), 1025–1028.
Chapple, W. M., & Forsyth, D. W. (1979). Earthquakes and bending of plates at trenches. *Journal of Geophysical Research*, *84*(B12), 6729–6749.
Cowie, P. A., & Scholz, C. H. (1992). Displacement-length scaling relationship for faults: Data synthesis and discussion. *Journal of Structural Geology*, *14*(10), 1149–1156.
Davies, J. H. (1999). The role of hydraulic fractures and intermediate depth earthquakes in generating subduction zone magmatism. *Nature*, *398*(6723), 142.
Di Giacomo, D., Bondár, I., Storchak, D. A., Engdahl, E. R., Bormann, P., & Harris, J. (2015). ISC-GEM: Global Instrumental Earthquake Catalogue (1900–2009), III. Re-computed MS and mb, proxy MW, final magnitude composition and completeness assessment. *Physics of the Earth and Planetary Interiors*, *239*, 33–47.
Emry, E. L., & Wiens, D. A. (2015). Incoming plate faulting in the Northern and Western Pacific and implications for subduction zone water budgets. *Earth and Planetary Science Letters*, *414*, 176–186.
Evans, J. P., Forster, C. B., & Goddard, J. V. (1997). Permeability of fault-related rocks, and implications for hydraulic structure of fault zones. *Journal of Structural Geology*, *19*(11), 1393–1404.
Faccenda, M., Burlini, L., Gerya, T. V., & Mainprice, D. (2008). Fault-induced seismic anisotropy by hydration in subducting oceanic plates. *Nature*, *455*(7216), 1097.
Faccenda, M., Gerya, T. V., & Burlini, L. (2009). Deep slab hydration induced by bending-related variations in tectonic pressure. *Nature Geoscience*, *2*(11), 790–793.
Faccenda, M., Gerya, T. V., Mancktelow, N. S., & Moresi, L. (2012). Fluid flow during slab unbending and dehydration: Implications for intermediate-depth seismicity, slab weakening and deep water recycling. *Geochemistry, Geophysics, Geosystems*, *13*, Q01010. https://doi.org/10.1029/2011GC003860
Faulkner, D., Mitchell, T., Jensen, E., & Cembrano, J. (2011). Scaling of fault damage zones with displacement and the implications for fault growth processes. *Journal of Geophysical Research*, *116*, B05403. https://doi.org/10.1029/2010JB007788
Ferrand, T. P., Hilairet, N., Incel, S., Deldicque, D., Labrousse, L., Gasc, J., et al. (2017). Dehydration-driven stress transfer triggers intermediate depth earthquakes. *Nature Communications*, *8*, 15247.
Gasc, J., Hilairet, N., Yu, T., Ferrand, T., Schubnel, A., & Wang, Y. (2017). Faulting of natural serpentinite: Implications for intermediate depth seismicity. *Earth and Planetary Science Letters*, *474*, 138–147.
Gorbatov, A., & Kostoglodov, V. (1997). Maximum depth of seismicity and thermal parameter of the subducting slab: General empirical relation and its application. *Tectonophysics*, *277*(1–3), 165–187.
Green, H. W., & Houston, H. (1995). The mechanics of deep earthquakes. *Annual Review of Earth and Planetary Sciences*, *23*(1), 169–213.
Grevemeyer, I., Ranero, C. R., Flueh, E. R., Kläschen, D., & Bialas, J. (2007). Passive and active seismological study of bending-related faulting and mantle serpentinization at the Middle America trench. *Earth and Planetary Science Letters*, *258*(3–4), 528–542.
Hacker, B. R. (2008). H2O subduction beyond arcs. *Geochemistry, Geophysics, Geosystems*, *9*, Q03001. https://doi.org/10.1029/2007GC001707
Hacker, B. R., Peacock, S. M., Abers, G. A., & Holloway, S. D. (2003). Subduction factory 2. Are intermediate-depth earthquakes in subducting slabs linked to metamorphic dehydration reactions? *Journal of Geophysical Research*, *108*(B1), 2030. https://doi.org/10.1029/2001JB001129
Hilde, T. W. (1983). Sediment subduction versus accretion around the Pacific. *Tectonophysics*, *99*(2–4), 381–397.
Hirth, G., & Guillot, S. (2013). Rheology and tectonic significance of serpentinite. *Elements*, *9*(2), 107–113.
Iyer, K., Rüpke, L. H., Phipps Morgan, J., & Grevemeyer, I. (2012). Controls of faulting and reaction kinetics on serpentinization and double Benioff zones. *Geochemistry, Geophysics, Geosystems*, *13*, Q09010. https://doi.org/10.1029/2012GC004304
Jamtveit, B., Putnis, C. V., & Malthe-Sørenssen, A. (2009). Reaction induced fracturing during replacement processes. *Contributions to Mineralogy and Petrology*, *157*(1), 127–133.
Jung, H., Fei, Y., Silver, P. G., & Green, H. W. (2009). Frictional sliding in serpentine at very high pressure. *Earth and Planetary Science Letters*, *277*(1), 273–279.
Jung, H., Green Ii, H. W., & Dobrzhinetskaya, L. F. (2004). Intermediate depth earthquake faulting by dehydration embrittlement with negative volume change. *Nature*, *428*(6982), 545–549.

Key, K., Constable, S., Matsuno, T., Evans, R. L., & Myer, D. (2012). Electromagnetic detection of plate hydration due to bending faults at the Middle America Trench. *Earth and Planetary Science Letters*, *351*, 45–53.
Kirby, S. H., Durham, W. B., & Stern, L. A. (1991). Mantle phase changes and deep-earthquake faulting in subducting lithosphere. *Science*, *252*(5003), 216–225. https://doi.org/10.1126/science.252.5003.216
Kirby, S. H., Stein, S., Okal, E. A., & Rubie, D. C. (1996). Metastable mantle phase transformations and deep earthquakes in subducting oceanic lithosphere. *Reviews of Geophysics*, *34*(2), 261–306.
Ludwig, W. J., Ewing, J. I., Ewing, M., Murauchi, S., Den, N., Asano, S., et al. (1966). Sediments and structure of the Japan Trench. *Journal of Geophysical Research*, *71*(8), 2121–2137.
Martin, B., & Fyfe, W. (1970). Some experimental and theoretical observations on the kinetics of hydration reactions with particular reference to serpentinization. *Chemical Geology*, *6*, 185–202.
Masson, D. (1991). Fault patterns at outer trench walls. *Marine Geophysical Researches*, *13*(3), 209–225.
Meade, C., & Jeanloz, R. (1991). Deep-focus earthquakes and recycling of water into the Earth's mantle. *Science*, *252*(5002), 68–72.
Michibayashi, K., Hirose, T., Nozaka, T., Harigane, Y., Escartin, J., Delius, H., et al. (2008). Hydration due to high-T brittle failure within in situ oceanic crust, 30 N Mid-Atlantic Ridge. *Earth and Planetary Science Letters*, *275*(3), 348–354.
Mitchell, T., & Faulkner, D. (2012). Towards quantifying the matrix permeability of fault damage zones in low porosity rocks. *Earth and Planetary Science Letters*, *339*, 24–31.
Molnar, P., Freedman, D., & Shih, J. S. (1979). Lengths of intermediate and deep seismic zones and temperatures in downgoing slabs of lithosphere. *Geophysical Journal International*, *56*(1), 41–54.
Naif, S., Key, K., Constable, S., & Evans, R. L. (2015). Water-rich bending faults at the Middle America Trench. *Geochemistry, Geophysics, Geosystems*, *16*, 2582–2597. https://doi.org/10.1002/2015GC005927
Nedimović, M. R., Bohnenstiehl, D. R., Carbotte, S. M., Canales, J. P., & Dziak, R. P. (2009). Faulting and hydration of the Juan de Fuca plate system. *Earth and Planetary Science Letters*, *284*(1–2), 94–102.
Nishikawa, T., & Ide, S. (2015). Background seismicity rate at subduction zones linked to slab-bending-related hydration. *Geophysical Research Letters*, *42*, 7081–7089. https://doi.org/10.1002/2015GL064578
Okazaki, K., & Hirth, G. (2016). Dehydration of lawsonite could directly trigger earthquakes in subducting oceanic crust. *Nature*, *530*(7588), 81–84.
Parsons, B., & Molnar, P. (1976). The origin of outer topographic rises associated with trenches. *Geophysical Journal International*, *45*(3), 707–712.
Peacock, S. A. (1990). Fluid processes in subduction zones. *Science*, *248*(4953), 329–337.
Peacock, S. M. (2001). Are the lower planes of double seismic zones caused by serpentine dehydration in subducting oceanic mantle? *Geology*, *29*(4), 299–302.
Pérez-Gussinyé, M., & Reston, T. J. (2001). Rheological evolution during extension at nonvolcanic rifted margins: Onset of serpentinization and development of detachments leading to continental breakup. *Journal of Geophysical Research*, *106*(B3), 3961–3975.
Plank, T., & Langmuir, C. H. (1998). The chemical composition of subducting sediment and its consequences for the crust and mantle. *Chemical Geology*, *145*(3), 325–394.
Pozgay, S. H., Wiens, D. A., Conder, J. A., Shiobara, H., & Sugioka, H. (2009). Seismic attenuation tomography of the Mariana subduction system: Implications for thermal structure, volatile distribution, and slow spreading dynamics. *Geochemistry, Geophysics, Geosystems*, *10*, Q04X05. https://doi.org/10.1029/2008GC002313
Proctor, B., & Hirth, G. (2016). "Ductile to brittle" transition in thermally stable antigorite gouge at mantle pressures. *Journal of Geophysical Research: Solid Earth*, *121*, 1652–1663. https://doi.org/10.1002/2015JB012710
Raleigh, C., & Paterson, M. (1965). Experimental deformation of serpentinite and its tectonic implications. *Journal of Geophysical Research*, *70*(16), 3965–3985.
Ranero, C. R., Morgan, J. P., McIntosh, K., & Reichert, C. (2003). Bending-related faulting and mantle serpentinization at the Middle America trench. *Nature*, *425*(6956), 367.
Ranero, C. R., & Sallares, V. (2004). Geophysical evidence for hydration of the crust and mantle of the Nazca plate during bending at the north Chile trench. *Geology*, *32*(7), 549–552.
Ranero, C. R., Villaseñor, A., Phipps Morgan, J., & Weinrebe, W. (2005). Relationship between bend-faulting at trenches and intermediate-depth seismicity. *Geochemistry, Geophysics, Geosystems*, *6*, Q12002. https://doi.org/10.1029/2005GC000997
Reynolds, S. J., & Lister, G. S. (1987). Structural aspects of fluid-rock interactions in detachment zones. *Geology*, *15*(4), 362–366.
Rüpke, L. H., & Hasenclever, J. (2017). Global rates of mantle serpentinization and H2 production at oceanic transform faults in 3-D geodynamic models. *Geophysical Research Letters*, *44*, 6726–6734. https://doi.org/10.1002/2017GL072893
Rüpke, L. H., Schmid, D. W., Perez-Gussinye, M., & Hartz, E. (2013). Interrelation between rifting, faulting, sedimentation, and mantle serpentinization during continental margin formation—Including examples from the Norwegian Sea. *Geochemistry, Geophysics, Geosystems*, *14*, 4351–4369. https://doi.org/10.1002/ggge.20268
Ryan, W. B., Carbotte, S. M., Coplan, J. O., O'Hara, S., Melkonian, A., Arko, R., et al. (2009). Global multi-resolution topography synthesis. *Geochemistry, Geophysics, Geosystems*, *10*, Q03014. https://doi.org/10.1029/2008GC002332
Savage, H. M., & Brodsky, E. E. (2011). Collateral damage: Evolution with displacement of fracture distribution and secondary fault strands in fault damage zones. *Journal of Geophysical Research*, *116*, B03405. https://doi.org/10.1029/2010JB007665
Scholz, C. H. (1987). Wear and gouge formation in brittle faulting. *Geology*, *15*(6), 493–495.
Schultz, R. A., Okubo, C. H., & Wilkins, S. J. (2006). Displacement-length scaling relations for faults on the terrestrial planets. *Journal of Structural Geology*, *28*(12), 2182–2193.
Shillington, D. J., Bécel, A., Nedimović, M. R., Kuehn, H., Webb, S. C., Abers, G. A., et al. (2015). Link between plate fabric, hydration and subduction zone seismicity in Alaska. *Nature Geoscience*, *8*(12), 961.
Shipton, Z., & Cowie, P. (2001). Damage zone and slip-surface evolution over μm to km scales in high-porosity Navajo sandstone, Utah. *Journal of Structural Geology*, *23*(12), 1825–1844.
Sibson, R. H. (2000). Fluid involvement in normal faulting. *Journal of Geodynamics*, *29*(3–5), 469–499.
Stern, R. J. (2002). Subduction zones. *Reviews of Geophysics*, *40*(4), 1012. https://doi.org/10.1029/2001RG000108
Syracuse, E. M., van Keken, P. E., & Abers, G. A. (2010). The global range of subduction zone thermal models. *Physics of the Earth and Planetary Interiors*, *183*(1), 73–90.
Tilmann, F. J., Grevemeyer, I., Flueh, E. R., Dahm, T., & Goßler, J. (2008). Seismicity in the outer rise offshore southern Chile: Indication of fluid effects in crust and mantle. *Earth and Planetary Science Letters*, *269*(1–2), 41–55.

Van Avendonk, H. J., Holbrook, W. S., Lizarralde, D., & Denyer, P. (2011). Structure and serpentinization of the subducting Cocos plate offshore Nicaragua and Costa Rica. *Geochemistry, Geophysics, Geosystems*, *12*, Q06009. https://doi.org/10.1029/2011GC003592
van Keken, P. E., Hacker, B. R., Syracuse, E. M., & Abers, G. A. (2011). Subduction factory: 4. Depth-dependent flux of H2O from subducting slabs worldwide. *Journal of Geophysical Research*, 116, B01401. https://doi.org/10.1029/2010JB007922
Wadati, K. (1928). Shallow and deep earthquakes. *Geophysical Magazine*, *1*, 162–202.
Warren, L. M., Hughes, A. N., & Silver, P. G. (2007). Earthquake mechanics and deformation in the Tonga-Kermadec subduction zone from fault plane orientations of intermediate- and deep-focus earthquakes. *Journal of Geophysical Research*, *112*, B05314. https://doi.org/10.1029/2006JB004677
Warren, L. M., Langstaff, M. A., & Silver, P. G. (2008). Fault plane orientations of intermediate-depth earthquakes in the Middle America Trench. *Journal of Geophysical Research*, *113*, B01304. https://doi.org/10.1029/2007JB005028
Wei, S. S., Wiens, D. A., van Keken, P. E., & Cai, C. (2017). Slab temperature controls on the Tonga double seismic zone and slab mantle dehydration. *Science Advances*, *3*(1), e1601755. https://doi.org/10.1126/sciadv.1601755
Wilkins, S. J., Schultz, R. A., Anderson, R. C., Dohm, J. M., & Dawers, N. H. (2002). Deformation rates from faulting at the Tempe Terra extensional province, Mars. *Geophysical Research Letters*, *29*(18), 1884. https://doi.org/10.1029/2002GL015391
Worzewski, T., Jegen, M., Kopp, H., Brasse, H., & Castillo, W. T. (2011). Magnetotelluric image of the fluid cycle in the Costa Rican subduction zone. *Nature Geoscience*, *4*(2), 108.
Yamasaki, T., & Seno, T. (2003). Double seismic zone and dehydration embrittlement of the subducting slab. *Journal of Geophysical Research*, *108*(B4), 2212. https://doi.org/10.1029/2002JB001918
Zhao, D., Wang, Z., Umino, N., & Hasegawa, A. (2007). Tomographic imaging outside a seismic network: Application to the northeast Japan arc. *Bulletin of the Seismological Society of America*, *97*(4), 1121–1132.

## References From the Supporting Information

Bilek, S. L., Schwartz, S. Y., & DeShon, H. R. (2003). Control of seafloor roughness on earthquake rupture behavior. *Geology*, *31*(5), 455–458.
Billen, M. I., & Gurnis, M. (2005). Constraints on subducting plate strength within the Kermadec trench. *Journal of Geophysical Research*, 110, B05407. https://doi.org/10.1029/2004JB003308
Bondár, I., Engdahl, E. R., Villaseñor, A., Harris, J., & Storchak, D. (2015). ISC-GEM: Global instrumental earthquake catalogue (1900–2009), II. Location and seismicity patterns. *Physics of the Earth and Planetary Interiors*, *239*, 2–13.
Bondár, I., & Storchak, D. (2011). Improved location procedures at the International Seismological Centre. *Geophysical Journal International*, *186*(3), 1220–1244.
Boston, B., Moore, G. F., Nakamura, Y., & Kodaira, S. (2014). Outer-rise normal fault development and influence on near-trench décollement propagation along the Japan Trench, off Tohoku. *Earth, Planets and Space*, *66*(1), 135.
Bouchon, M., Marsan, D., Durand, V., Campillo, M., Perfettini, H., Madariaga, R., & Gardonio, B. (2016). Potential slab deformation and plunge prior to the Tohoku, Iquique and Maule earthquakes. *Nature Geoscience*, *9*(5), 380.
Faccenna, C., Holt, A. F., Becker, T. W., Lallemand, S., & Royden, L. H. (2018). Dynamics of the Ryukyu/Izu-Bonin-Marianas double subduction system. *Tectonophysics*, *746*, 229–238.
Han, S., Carbotte, S. M., Canales, J. P., Nedimović, M. R., Carton, H., Gibson, J. C., & Horning, G. W. (2016). Seismic reflection imaging of the Juan de Fuca plate from ridge to trench: New constraints on the distribution of faulting and evolution of the crust prior to subduction. *Journal of Geophysical Research: Solid Earth*, *121*, 1849–1872. https://doi.org/10.1002/2015JB012416
International Seismological Centre (2015). On-line Bulletin.
Kimura, G., Hashimoto, Y., Kitamura, Y., Yamaguchi, A., & Koge, H. (2014). Middle Miocene swift migration of the TTT triple junction and rapid crustal growth in southwest Japan: A review. *Tectonics*, *33*, 1219–1238. https://doi.org/10.1002/2014TC003531
Massell, C. G. (2002). Large-scale structural variation of trench outer slopes and rises.
Miller, M. S., Gorbatov, A., & Kennett, B. L. N. (2005). Heterogeneity within the subducting Pacific slab beneath the Izu–Bonin–Mariana arc: Evidence from tomography using 3D ray tracing inversion techniques. *Earth and Planetary Science Letters*, *235*(1–2), 331–342.
Nakamura, Y., Kodaira, S., Cook, B. J., Jeppson, T., Kasaya, T., Yamamoto, Y., et al. (2014). Seismic imaging and velocity structure around the JFAST drill site in the Japan Trench: Low V p, high V p/V s in the transparent frontal prism. *Earth, Planets and Space*, *66*(1), 121.
Naliboff, J. B., Billen, M. I., Gerya, T., & Saunders, J. (2013). Dynamics of outer-rise faulting in oceanic-continental subduction systems. *Geochemistry, Geophysics, Geosystems*, *14*, 2310–2327. https://doi.org/10.1002/ggge.20155
Uyeda, S., & Ben-Avraham, Z. (1972). Origin and development of the Philippine Sea. *Nature Physical Science*, *240*(104), 176.
Van der Hilst, R., Widiyantoro, S., & Engdahl, E. (1997). Evidence for deep mantle circulation from global tomography. *Nature*, *386*(6625), 578.
Zhou, Z., Lin, J., Behn, M. D., & Olive, J. A. (2015). Mechanism for normal faulting in the subducting plate at the Mariana Trench. *Geophysical Research Letters*, *42*, 4309–4317. https://doi.org/10.1002/2015GL063917